Progress of Theoretical Physics, Vol. 37, No. 4, April 1967

Ground State Energy Difference of Hcp and Fcc Ortho-Hydrogens*)

Hiroshi MIYAGI and Tuto NAKAMURA

Faculty of Engineering Science, Osaka University, Toyonaka

(Received November 17, 1966)

The lowest state of the quadrupole-quadrupole interaction is studied for hcp and fcc ortho-hydrogens. The difference of the classical ground state energies of hcp and fcc ortho-hydrogens is estimated to be 0.72 °K per molecule by use of the previous result for the fcc structure given by one of us. The zero-point energy corrections are studied also for both hcp and fcc structures by a perturbation calculation. The resulting ground state energy difference is estimated to be 0.57 °K per molecule

§ 1. Introduction

By observing the infrared spectrum, Clouter and Gush[1] found recently that the structure of solid normal hydrogen changes from a hexagonal close-packed structure (hcp) to a structure with inversion symmetry around 1.4°K. Mills and Schuch[2] confirmed this structure change by observing X-ray photographs. They found that the structure is hcp from 4°K to 1.3°K and transforms below 1.3°K to a face-centered cubic structure (fcc). They found also that the transition temperature decreases with decreasing ortho-para ratio. This is consistent with the established result that the structure of solid para-hydrogen is hcp.[3),4)]

The transition would be related closely to the removal of the three-fold degeneracy at rotational states of ortho-molecules with rotational quantum number equal to one. The removal of the degeneracy has been confirmed by observations of the specific heat anomaly[5),6)] and of the line shape change in nuclear magnetic resonance.[7),8)] The interaction responsible for the removal comes mainly from the quadrupole-quadrupole interaction between ortho-molecules, as was shown by analyzing the anomalous specific heat.[9)] This is also the case for solid deuterium.[10)]

Thus the ordered orientation of molecules in solid ortho-hydrogen would be in the lowest state of the quadrupole-quadrupole interaction between molecules. For fcc this lowest state has been obtained classically by Nagai and Nakamura,[11)] generalizing Luttinger and Tisza's method.[12)] The hcp-fcc transition occurring in solid hydrogen with higher concentrations of ortho-molecules means that the ordering energy would be larger for fcc than for hcp. Hence it is interesting

*) Read at the Annual Meeting of the Physical Society of Japan, April, 1966.

to see how much the ground state energy difference of the quadrupole interaction for hcp and fcc is. To get this energy difference the ground state energy for hcp is needed.

Several attempts have been made to find the ordered molecular configuration in hcp. Danielian[13] proposed an ordered configuration of ortho-hydrogen with a lower energy in comparison with the configuration assumed in the previous works.[14),15] Kitaigorodskii and Mirskaya[16] examined the classical quadrupole energies for some symmetrical arrangements of molecules in hcp. Felsteiner[17] gave a lower limit for the lowest classical energy of quadrupoles in hcp. However, it seems that there is no systematic examination of the quadrupole arrangements in hcp. In §§ 2 and 3 of the present paper, we shall give a detailed examination of them, following the method given in the previous paper.[11]

As shown by Raich and James,[18] the ground state energy of solid ortho-hydrogen is estimated from that of the classical quadrupole system with a conversion factor $(2/5)^2$. The resulting estimate is a semiclassical value. There may be some correction to that, coming from the zero-point energy. This effect would be studied by looking into the rotational excitation in the ordered state,[19] as seen in the spin wave theory of ordered magnets. We shall treat the zero-point correction to the ground state energy by a perturbation calculation for both fcc and hcp ortho-hydrogens. The result will be given in § 4.

§ 2. Characteristic quadrupole arrays in hcp crystals

The quadrupole interaction between two molecules with distance R is written

$$V=\frac{3e^2\mu_Q^2}{16R^5}\left\{1+2(\boldsymbol{s}_1\cdot\boldsymbol{s}_2)^2-5\frac{(\boldsymbol{s}_1\cdot\boldsymbol{R})^2+(\boldsymbol{s}_2\cdot\boldsymbol{R})^2}{R^2}\right.$$
$$\left.-20\frac{(\boldsymbol{s}_1\cdot\boldsymbol{R})(\boldsymbol{s}_2\cdot\boldsymbol{R})}{R^2}(\boldsymbol{s}_1\cdot\boldsymbol{s}_2)+35\frac{(\boldsymbol{s}_1\cdot\boldsymbol{R})^2(\boldsymbol{s}_2\cdot\boldsymbol{R})^2}{R^4}\right\}, \tag{2·1}$$

where $\boldsymbol{R}$ is the vector connecting the centers of two quadrupoles, $e\mu_Q$ the electric quadrupole moment of molecule, and $\boldsymbol{s}_1$ and $\boldsymbol{s}_2$ are the unit vectors representing the directions of molecular axes. If we denote the direction cosines of $\boldsymbol{s}$ by (ξ, η, ζ), the quadrupole interaction (2·1) summed over all pairs of molecules can be written

$$W=\sum_{j>k}\sum_{\mu,\nu} z_\mu^j F_{\mu\nu}(\boldsymbol{R}_j-\boldsymbol{R}_k) z_\nu^k. \tag{2·2}$$

Here z_μ^j denotes the μ-th quadrupole component of the j-th molecule with the position vector $\boldsymbol{R}_j$. Five components of the quadrupole are given in the column (a) of Table I and $F_{\mu\nu}(\boldsymbol{R})$'s in Table II.*)

The lowest energy configuration of the classical quadrupole system in hcp

*) Figures given in Table II differ by a factor 2 from those in Table I of reference 11), as was reported in the Errata.

Table I. Quadrupole components.

	(a)	(b)
z_1	$\frac{\sqrt{3}}{2}(\xi^2-\eta^2)$	$-\frac{2}{5}\times\frac{\sqrt{3}}{2}(J_\xi^2-J_\eta^2)$
z_2	$\frac{1}{2}(3\zeta^2-1)$	$-\frac{2}{5}\times\frac{1}{2}(3J_\zeta^2-2)$
z_3	$\sqrt{3}\,\eta\zeta$	$-\frac{2}{5}\times\frac{\sqrt{3}}{2}(J_\eta J_\zeta+J_\zeta J_\eta)$
z_4	$\sqrt{3}\,\zeta\xi$	$-\frac{2}{5}\times\frac{\sqrt{3}}{2}(J_\zeta J_\xi+J_\xi J_\zeta)$
z_5	$\sqrt{3}\,\xi\eta$	$-\frac{2}{5}\times\frac{\sqrt{3}}{2}(J_\xi J_\eta+J_\eta J_\xi)$

(ξ, η, ζ) are the direction cosines of molecule.
J_ξ, J_η and J_ζ are the angular momentum operators with $J=1$.

Tabe II. Expressions for $F_{\mu\nu}(\boldsymbol{R})\times(4R^5/3e^2\mu_Q^2)$.

μ	ν	$P_4^0(\cos\Theta)$	$P_4^2(\cos\Theta)$		$P_4^4(\cos\Theta)$	
			$\cos 2\Phi$	$\sin 2\Phi$	$\cos 4\Phi$	$\sin 4\Phi$
1	1	4/3			1/18	
1	2		$2/3\sqrt{3}$			
1	5					1/18
2	2	8				
2	5			$2/3\sqrt{3}$		
3	3	−16/3	−4/9			
3	4			4/9		
4	4	−16/3	4/9			
5	5	4/3			−1/18	

μ	ν	$P_4^1(\cos\Theta)$		$P_4^3(\cos\Theta)$	
		$\cos\Phi$	$\sin\Phi$	$\cos 3\Phi$	$\sin 3\Phi$
1	3		2/3		1/9
1	4	−2/3		1/9	
2	3		$4/\sqrt{3}$		
2	4	$4/\sqrt{3}$			
3	5	−2/3		−1/9	
4	5		−2/3		1/9

(Θ, Φ) denote the polar and azimuthal angles of the direction $\boldsymbol{R}$.

will be studied by the same method as given in reference 11), namely by a generalized Luttinger and Tisza's method. We first look for the lowest energy configuration of quadrupoles by minimizing (2·2) with a subsidiary condition

$$\sum_i \sum_\mu (z_\mu{}^i)^2 = N. \tag{2·3}$$

This condition comes from

$$\sum_\mu (z_\mu{}^i)^2 = 1 \tag{2·4}$$

summed over all molecules. Owing to translational symmetry, the solution would be a periodic pattern composed of

$$z_\mu(\boldsymbol{\lambda}) \exp(-i\boldsymbol{\lambda}\cdot\boldsymbol{R}_j). \tag{2·5}$$

Here $z_\mu(\boldsymbol{\lambda})$ denotes the amplitude of the μ-th quadrupole component with a spatial variation $\exp(-i\boldsymbol{\lambda}\cdot\boldsymbol{R}_j)$. The energy minimum condition leads to

$$\sum_\nu \{\sum_k F_{\mu\nu}(\boldsymbol{R}_j - \boldsymbol{R}_k) \exp(i\boldsymbol{\lambda}\cdot(\boldsymbol{R}_j - \boldsymbol{R}_k))\} z_\nu(\boldsymbol{\lambda}) = f z_\mu(\boldsymbol{\lambda}). \tag{2·6}$$

The eigenvalue f of the above eigenvalue problem turns out to be twice the quadrupole energy per molecule. If we multiply both sides of (2·6) by $\exp(-i\boldsymbol{\lambda}\cdot\boldsymbol{R}_j)$, the left-hand side of the resulting equation represents the μ-th component of the quadrupole field at the j-th site owing to quadrupoles at the other sites. Hence (2·6) means that the quadrupole field 'vector' at a lattice site would be parallel to the quadrupole 'vector' at the same site. The proportional constant is f, which will be referred to as field value.

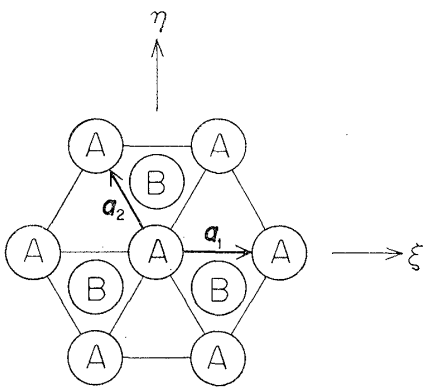

Fig. 1. Coordinate system. The basic vectors are $\boldsymbol{a}_1$, $\boldsymbol{a}_2$ and $\boldsymbol{c}$, where $\boldsymbol{c}$ is perpendicular to $\boldsymbol{a}_1$ and $\boldsymbol{a}_2$, $|\boldsymbol{a}_1| = |\boldsymbol{a}_2| = a$ and $|\boldsymbol{c}| = c = \sqrt{8/3}\ a$.

If the eigenvector belonging to the lowest field value gives a real molecular configuration, everything would be right. However, this is not always the case. It is because our formalism is based on a weak condition (2·3). If we could not find real direction cosines (ξ_i, η_i, ζ_i) from the lowest eigenvector, this vector represents a fictitious quadrupole configuration. However, any real molecular configuration would be represented by some linear combination of eigenvectors. The eigenvectors of (2·6) will be called characteristic quadrupole arrays. The lowest characteristic quadrupole array is fictitious in hcp and real in fcc.

The coordinate system shown in Fig. 1 is taken to represent the position vector $\boldsymbol{R}_j$, whose distance is measured in units of a, distance to nearest neighbors. It is to be noted that the unit cell in hcp includes two lattice points, namely (0, 0, 0) and $(\frac{1}{3}, -\frac{1}{3}, \frac{1}{2})$ in our coordinate system. Then we divide the lattice into two sublattices, A and B, as shown in Fig. 1.

We first study the quadrupole arrays with $\boldsymbol{\lambda} = (0, 0, 0)$, that is the uniform array in each sublattice. For the uniform arrays, there is no field component at a lattice site, coming from different components of quadrupoles in the lattice.

Then we have field values given by

$$\begin{pmatrix} f_\mu \\ \tilde{f}_\mu \end{pmatrix} = \sum_{k(\neq j)} F^{\mathrm{AA}}_{\mu\mu}(\boldsymbol{R}_j - \boldsymbol{R}_k) \begin{pmatrix} + \\ - \end{pmatrix} \sum_l F^{\mathrm{AB}}_{\mu\mu}(\boldsymbol{R}_j - \boldsymbol{R}_l)$$

$$\mu = 1, 2, \cdots, 5, \tag{2·7}$$

where the lattice points j and k belong to A-lattice and l to B-lattice. Two kinds of field values, f_μ and $\tilde{f}_\mu$, come from two different types of uniform arrays. If we define a basic vector $\boldsymbol{z}_\mu$ by

$$\text{the } \mu\text{-th component of } \boldsymbol{z}_\mu = 1$$

$$\text{and the other components of } \boldsymbol{z}_\mu = 0, \tag{2·8}$$

f_μ and $\tilde{f}_\mu$ are the field values associated with $(\boldsymbol{z}_\mu, \boldsymbol{z}_\mu)$ and $(\boldsymbol{z}_\mu, -\boldsymbol{z}_\mu)$ respectively. Here, two vectors in $(\boldsymbol{z}_\mu, \boldsymbol{z}_\mu)$ or $(\boldsymbol{z}_\mu, -\boldsymbol{z}_\mu)$ refer to quadrupole vectors in A- and B-lattices respectively.

Table III. Field values of the uniform characteristic array.

Even type		Odd type	
Characteristic array	Field value f_μ^0	Characteristic array	Field value $\tilde{f}_\mu^0$
$\boldsymbol{Z}_1^0(\boldsymbol{z}_1, \boldsymbol{z}_1)$	$1.20g$	$\tilde{\boldsymbol{Z}}_1^0(\boldsymbol{z}_1, -\boldsymbol{z}_1)$	$5.60\,g$
$\boldsymbol{Z}_2^0(\boldsymbol{z}_2, \boldsymbol{z}_2)$	7.22	$\tilde{\boldsymbol{Z}}_2^0(\boldsymbol{z}_2, -\boldsymbol{z}_2)$	33.58
$\boldsymbol{Z}_3^0(\boldsymbol{z}_3, \boldsymbol{z}_3)$	-4.82	$\tilde{\boldsymbol{Z}}_3^0(\boldsymbol{z}_3, -\boldsymbol{z}_3)$	-22.38
$\boldsymbol{Z}_4^0(\boldsymbol{z}_4, \boldsymbol{z}_4)$	-4.82	$\tilde{\boldsymbol{Z}}_4^0(\boldsymbol{z}_4, -\boldsymbol{z}_4)$	-22.38
$\boldsymbol{Z}_5^0(\boldsymbol{z}_5, \boldsymbol{z}_5)$	1.20	$\tilde{\boldsymbol{Z}}_5^0(\boldsymbol{z}_5, -\boldsymbol{z}_5)$	5.60

Field values of the uniform characteristic array are given in Table III, where we measure the field value f in units of

$$g = 3e^2\mu_Q^2/4a^5\,. \tag{2·9}$$

The numerical value of g is 2.82×10^{-16} erg or $2.04\,^\circ$K. Lattice sums in (2·7) have been evaluated by Ewald and Kornfeld's method.

We next study quadrupole arrays with $\boldsymbol{\lambda} = (0, \pi, 0)$. With this translational symmetry, the first component of quadrupole 'vector' in the array gives rise to the second component of quadrupolar field at a lattice site. Incidently the characteristic quadrupole arrays connected with $\boldsymbol{z}_1$ and $\boldsymbol{z}_2$ come out as linear combinations of $\boldsymbol{z}_1$ and $\boldsymbol{z}_2$. The results are shown in Table IV. The phase of quadrupole 'vector' in B-lattice relative to that in A-lattice is chosen as illustrated in the figures given there.

The field values of quadrupole arrays with $\boldsymbol{\lambda} = (0, \pi, 0)$ are threefold degenerate. This degeneracy comes from the fact that the arrays considered have a threefold rotational symmetry axis around c-axis. If we rotate a pattern of $(0, \pi, 0)$ arrays be $2\pi/3$ around c-axis, the pattern to come out will represent the array with $\boldsymbol{\lambda} = (\pi, 0, 0)$. In the same way, we can get arrays with $\boldsymbol{\lambda} = (\pi, \pi, 0)$ from those with $\boldsymbol{\lambda} = (0, \pi, 0)$ by the rotation of $-2\pi/3$ around c-axis.

Table IV. Field values and characteristic quadrupole arrays with $\boldsymbol{\lambda}=(0,\ \pi,\ 0)$.

Even type

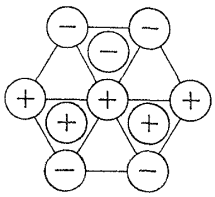

Odd type

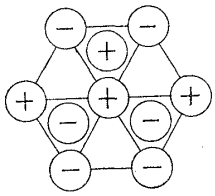

Characteristic array	Vector at the origin	Field value f_μ'	Characteristic array	Vector at the origin	Field value $\tilde{f}_\mu'$
$\boldsymbol{Z}_1'$	$\gamma_2 \boldsymbol{z}_1+\gamma_1 \boldsymbol{z}_2$	23.51 g	$\tilde{\boldsymbol{Z}}_1'$	$\delta_2 \boldsymbol{z}_1+\delta_1 \boldsymbol{z}_2$	38.88 g
$\boldsymbol{Z}_2'$	$-\gamma_1 \boldsymbol{z}_1+\gamma_2 \boldsymbol{z}_2$	− 5.13	$\tilde{\boldsymbol{Z}}_2'$	$-\delta_1 \boldsymbol{z}_1+\delta_2 \boldsymbol{z}_2$	−18.26
$\boldsymbol{Z}_3'$	$\boldsymbol{z}_3$	− 1.62	$\tilde{\boldsymbol{Z}}_3'$	$\boldsymbol{z}_3$	31.22
$\boldsymbol{Z}_4'$	$\boldsymbol{z}_4$	7.70	$\tilde{\boldsymbol{Z}}_4'$	$\boldsymbol{z}_4$	−25.14
$\boldsymbol{Z}_5'$	$\boldsymbol{z}_5$	−24.48	$\tilde{\boldsymbol{Z}}_5'$	$\boldsymbol{z}_5$	−26.72

The characteristic quadrupole array is defined by a set of quadrupoles with 'vector' given in the second column, where each vector has + or − sign as designated in respective figures. In the table $\gamma_1^2+\gamma_2^2=\delta_1^2+\delta_2^2=1$, $(\gamma_1,\gamma_2)=(-0.141,\ 0.990)$ and $(\delta_1,\ \delta_2)=(0.490,\ 0.872)$.

Table V. Characteristic quadrupole arrays with $\boldsymbol{\lambda}=(\pi,\ 0,\ 0)$ and $\boldsymbol{\lambda}=(\pi,\ \pi,\ 0)$.

(a) $\boldsymbol{\lambda}=(\pi,\ 0,\ 0)$

Even type		Odd type	
Characteristic array	Vector at the origin	Characteristic array	Vector at the origin
$\boldsymbol{Z}_1''$	$\gamma_2\{-(1/2)\boldsymbol{z}_1-(\sqrt{3}/2)\boldsymbol{z}_5\}+\gamma_1\boldsymbol{z}_2$	$\tilde{\boldsymbol{Z}}_1''$	$\delta_2\{-(1/2)\boldsymbol{z}_1-(\sqrt{3}/2)\boldsymbol{z}_5\}+\delta_1\boldsymbol{z}_2$
$\boldsymbol{Z}_2''$	$-\gamma_1\{-(1/2)\boldsymbol{z}_1-(\sqrt{3}/2)\boldsymbol{z}_5\}+\gamma_2\boldsymbol{z}_2$	$\tilde{\boldsymbol{Z}}_2''$	$-\delta_1\{-(1/2)\boldsymbol{z}_1-(\sqrt{3}/2)\boldsymbol{z}_5\}+\delta_2\boldsymbol{z}_2$
$\boldsymbol{Z}_3''$	$-(1/2)\boldsymbol{z}_3-(\sqrt{3}/2)\boldsymbol{z}_4$	$\tilde{\boldsymbol{Z}}_3''$	$-(1/2)\boldsymbol{z}_3-(\sqrt{3}/2)\boldsymbol{z}_4$
$\boldsymbol{Z}_4''$	$(\sqrt{3}/2)\boldsymbol{z}_3-(1/2)\boldsymbol{z}_4$	$\tilde{\boldsymbol{Z}}_4''$	$(\sqrt{3}/2)\boldsymbol{z}_3-(1/2)\boldsymbol{z}_4$
$\boldsymbol{Z}_5''$	$(\sqrt{3}/2)\boldsymbol{z}_1-(1/2)\boldsymbol{z}_5$	$\tilde{\boldsymbol{Z}}_5''$	$(\sqrt{3}/2)\boldsymbol{z}_1-(1/2)\boldsymbol{z}_5$

(b) $\boldsymbol{\lambda}=(\pi,\ \pi,\ 0)$

Even type		Odd type	
Characteristic array	Vector at the origin	Characteristic array	Vector at the origin
$\boldsymbol{Z}_1'''$	$\gamma_2\{-(1/2)\boldsymbol{z}_1+(\sqrt{3}/2)\boldsymbol{z}_5\}+\gamma_1\boldsymbol{z}_2$	$\tilde{\boldsymbol{Z}}_1'''$	$\delta_2\{-(1/2)\boldsymbol{z}_1+(\sqrt{3}/2)\boldsymbol{z}_5\}+\delta_1\boldsymbol{z}_2$
$\boldsymbol{Z}_2'''$	$-\gamma_1\{-(1/2)\boldsymbol{z}_1+(\sqrt{3}/2)\boldsymbol{z}_5\}+\gamma_2\boldsymbol{z}_2$	$\tilde{\boldsymbol{Z}}_2'''$	$-\delta_1\{-(1/2)\boldsymbol{z}_1+(\sqrt{3}/2)\boldsymbol{z}_5\}+\delta_2\boldsymbol{z}_2$
$\boldsymbol{Z}_3'''$	$-(1/2)\boldsymbol{z}_3+(\sqrt{3}/2)\boldsymbol{z}_4$	$\tilde{\boldsymbol{Z}}_3'''$	$-(1/2)\boldsymbol{z}_3+(\sqrt{3}/2)\boldsymbol{z}_4$
$\boldsymbol{Z}_4'''$	$-(\sqrt{3}/2)\boldsymbol{z}_3-(1/2)\boldsymbol{z}_4$	$\tilde{\boldsymbol{Z}}_4'''$	$-(\sqrt{3}/2)\boldsymbol{z}_3-(1/2)\boldsymbol{z}_4$
$\boldsymbol{Z}_5'''$	$-(\sqrt{3}/2)\boldsymbol{z}_1-(1/2)\boldsymbol{z}_5$	$\tilde{\boldsymbol{Z}}_5'''$	$-(\sqrt{3}/2)\boldsymbol{z}_1-(1/2)\boldsymbol{z}_5$

By $\boldsymbol{Z}_\mu''$ we designate a new 'vector' generated from $\boldsymbol{Z}_\mu'$ given in Table IV, by the rotation of $2\pi/3$. In Table V, we give a quadrupole 'vector' at the origin for the characteristic array $\boldsymbol{Z}_\mu''$. This vector generates the whole arrays in the lattice according to $(+, -)$-pattern obtained from the pattern given in Table IV by the rotation of $2\pi/3$. The corresponding 'vectors' generated by the rotation of $-2\pi/3$ are also given in Table V. $\boldsymbol{Z}_\mu'$, $\boldsymbol{Z}_\mu''$ and $\boldsymbol{Z}_\mu'''$ are degenerate in a field value f_μ'.

We have studied quadrupole arrays with other various symmetries. Some results are given briefly in § 5. The lowest field value has proved to be $-26.72\,g$, whose characteristic quadrupole arrays are $\tilde{\boldsymbol{Z}}_5'$, $\tilde{\boldsymbol{Z}}_5''$ and $\tilde{\boldsymbol{Z}}_5'''$ as given in Tables IV and V. This field value was reported also by Felsteiner.[17] Any linear combination of the above three degenerate arrays cannot give real quadrupole array. In order to get the real array we should take into account characteristic arrays with higher field values. Thus one half of the lowest field value gives a lower limit of the quadrupole energy per molecule in hcp. This lower limit is higher than the quadrupole energy per molecule in fcc, that is $-28.46\,g/2$.

§ 3. Construction of the lowest real quadrupole array

The lowest characteristic quadrupole array is fictitious in hcp, as mentioned in § 2. We shall find the lowest real quadrupole array by making a linear combination of the characteristic quadrupole arrays. We do this in a manifold spun by the characteristic vectors with $\boldsymbol{\lambda}=(0, 0, 0)$, $(0, \pi, 0)$, $(\pi, 0, 0)$ and $(\pi, \pi, 0)$. This procedure is equivalent to finding the lowest quadrupole configuration in the 8-sublattice model. The characteristic quadrupole array will hereafter be represented by 8 quadrupole vectors, that is an 8×5 dimensional vector.

A real quadrupole array $\boldsymbol{Z}$, and 8×5 dimensional 'vector', is decomposed into the characteristic arrays as follows:

$$\boldsymbol{Z}=\sum_\mu\sum_m a_\mu^{(m)}\boldsymbol{Z}_\mu^{(m)}+\sum_\mu\sum_m \tilde{a}_\mu^{(m)}\tilde{\boldsymbol{Z}}_\mu^{(m)}, \tag{3·1}$$

where $(m)=0$ refers to the uniform array and $(m)=', ''$ and $'''$ to $\boldsymbol{\lambda}=(0, \pi, 0)$, $(\pi, 0, 0)$ and $(\pi, \pi, 0)$ respectively. We note that the characteristic vectors are orthogonal:

$$\begin{aligned}&(\boldsymbol{Z}_\mu^{(m)}, \boldsymbol{Z}_\nu^{(n)})=(\tilde{\boldsymbol{Z}}_\mu^{(m)}, \tilde{\boldsymbol{Z}}_\nu^{(n)})=8\delta_{\mu\nu}\delta_{mn},\\&(\boldsymbol{Z}_\mu^{(m)}, \tilde{\boldsymbol{Z}}_\nu^{(n)})=0.\end{aligned} \tag{3·2}$$

Here we normalized $\boldsymbol{Z}$ as $(\boldsymbol{Z}, \boldsymbol{Z})=8$. Then

$$\sum_\mu\sum_m|a_\mu^{(m)}|^2+\sum_\mu\sum_m|\tilde{a}_\mu^{(m)}|^2=1. \tag{3·3}$$

The quadrupole field vector $\boldsymbol{F}$, an 8×5 dimensional vector, associated with the array $\boldsymbol{Z}$ is written

$$\boldsymbol{F}=\sum_{\mu}\sum_{m}a_{\mu}^{(m)}f_{\mu}^{(m)}\boldsymbol{Z}_{\mu}^{(m)}+\sum_{\mu}\sum_{m}\tilde{a}_{\mu}^{(m)}\tilde{f}_{\mu}^{(m)}\tilde{\boldsymbol{Z}}_{\mu}^{(m)}, \tag{3·4}$$

if we remember the field associated with each characteristic array to be parallel to the characteristic vector with a proportional constant $f_{\mu}^{(m)}$ or $\tilde{f}_{\mu}^{(m)}$. Making a scalar product of $\boldsymbol{F}$ and $\boldsymbol{Z}$, $(\boldsymbol{F}, \boldsymbol{Z})$, and using (3·2), we have

$$f=\sum_{\mu}\sum_{m}|a_{\mu}^{(m)}|^{2}f_{\mu}^{(m)}+\sum_{\mu}\sum_{m}|\tilde{a}_{\mu}^{(m)}|^{2}\tilde{f}_{\mu}^{(m)}, \tag{3·5}$$

where $\frac{1}{8}(\boldsymbol{F}, \boldsymbol{Z})=f$ is an average field value. This average field value will be referred to also as field value.

To get the lowest real quadrupole array, we need to fix the above expansion coefficients, $a_{\mu}^{(m)}$ and $\tilde{a}_{\mu}^{(m)}$, so as to make satisfy two different kinds of conditions, the extremum condition and the reality condition of quadrupole.

We first give the extremum condition. Let $\boldsymbol{f}$ be a quadrupole field acting on a quadrupole $\boldsymbol{z}$ in the lattice, both $\boldsymbol{f}$ and $\boldsymbol{z}$ being five dimensional vectors. If the quadrupole $\boldsymbol{z}$ is in an extremum configuration under the field $\boldsymbol{f}$, then no infinitesimal rotation of molecule gives rise to any change in the quadrupole energy $(\boldsymbol{f}, \boldsymbol{z})$. This condition is written down

$$(\boldsymbol{f}, L_{\xi}\boldsymbol{z})=(\boldsymbol{f}, L_{\eta}\boldsymbol{z})=(\boldsymbol{f}, L_{\zeta}\boldsymbol{z})=0, \tag{3·6}$$

where L_{ξ}, L_{η} and L_{ζ} are the infinitesimal rotation operators around ξ-, η- and ζ-axes respectively; for example,

$$L_{\xi}=-i\left(\eta\frac{\partial}{\partial\zeta}-\zeta\frac{\partial}{\partial\eta}\right).$$

The matrix representations for these operators are given by

$$L_{\xi}=\begin{pmatrix} 0 & 0 & i & 0 & 0 \\ 0 & 0 & i\sqrt{3} & 0 & 0 \\ -i & -i\sqrt{3} & 0 & 0 & 0 \\ 0 & 0 & 0 & 0 & i \\ 0 & 0 & 0 & -i & 0 \end{pmatrix},$$

$$L_{\eta}=\begin{pmatrix} 0 & 0 & 0 & i & 0 \\ 0 & 0 & 0 & -i\sqrt{3} & 0 \\ 0 & 0 & 0 & 0 & -i \\ -i & i\sqrt{3} & 0 & 0 & 0 \\ 0 & 0 & i & 0 & 0 \end{pmatrix}$$

and

$$L_\zeta = \begin{pmatrix} 0 & 0 & 0 & 0 & -2i \\ 0 & 0 & 0 & 0 & 0 \\ 0 & 0 & 0 & i & 0 \\ 0 & 0 & -i & 0 & 0 \\ 2i & 0 & 0 & 0 & 0 \end{pmatrix}, \tag{3·7}$$

where our bases of quadrupole, z_1, z_2, z_3, z_4 and z_5, are taken as bases of the above representation in the same order. Then the extremum conditions (3·6) are written

$$\begin{aligned} &(z_1 f_3 - z_3 f_1) + \sqrt{3}(z_2 f_3 - z_3 f_2) + (z_4 f_5 - z_5 f_4) = 0, \\ &(z_1 f_4 - z_4 f_1) + \sqrt{3}(z_4 f_2 - z_2 f_4) + (z_5 f_3 - z_3 f_5) = 0, \\ &2(z_5 f_1 - z_1 f_5) + (z_3 f_4 - z_4 f_3) = 0, \end{aligned} \tag{3·8}$$

where $f_1, \cdots, f_5$ are five components of $\boldsymbol{f}$. Only two of (3·8) are independent conditions. The condition (3·8) would be satisfied for all molecular sites in the extremum configuration. It is to be noted that the condition is automatically satisfied in the case when $\boldsymbol{f}$ is parallel to $\boldsymbol{z}$. This is the case for characteristic quadrupole arrays.

We next give the reality condition of quadrupole. Of five quadrupole components we have only two independent components; we have three conditions for each quadrupole, one of which is given by (2·4). The others are written

$$\begin{aligned} &z_3^2 - z_4^2 = (2/\sqrt{3}) z_1 (1 + 2z_2), \\ &z_3 z_4 = (1/\sqrt{3}) z_5 (1 + 2z_2). \end{aligned} \tag{3·9}$$

From these conditions we have

$$\begin{aligned} &z_3 = \pm (1/\sqrt{3}) \{(1 - z_2 - \sqrt{3} z_1)(1 + 2z_2)\}^{1/2}, \\ &z_4 = \pm (1/\sqrt{3}) \{(1 - z_2 + \sqrt{3} z_1)(1 + 2z_2)\}^{1/2}, \\ &z_5 = \pm (1/\sqrt{3}) \{(1 - z_2)^2 - 3z_1^2\}^{1/2}. \end{aligned} \tag{3·10}$$

One of signs in the above expressions for z_3, z_4 and z_5 is chosen respectively in the following combinations.

$$\begin{bmatrix} + \\ + \\ + \end{bmatrix}, \begin{bmatrix} + \\ - \\ - \end{bmatrix}, \begin{bmatrix} - \\ + \\ - \end{bmatrix} \text{and} \begin{bmatrix} - \\ - \\ + \end{bmatrix}. \tag{3·11}$$

The other sign combinations do not appear in the real quadrupole, as easily seen from Table I. The allowed region of z_1 and z_2 is shown in Fig. 2. If we distribute the above sign combinations over the 8 lattice points, we would have 4^7 different configurations for fixed z_1 and z_2 over the 8 lattice points.

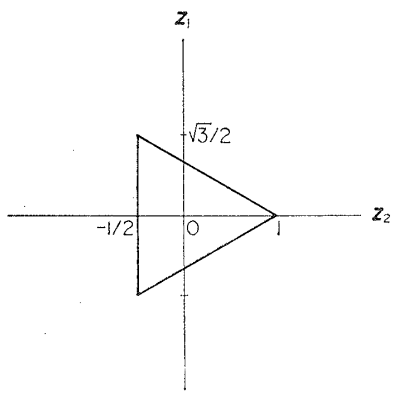

Fig. 2. Allowed region in the z_2, z_1-plane.

We construct real quadrupole arrays satisfying the extremum condition, where symmetric arrangements of quadrupoles are assumed. Actually we examine the extremum condition only for a few types of symmetric arrangements. Because we can get a rough estimate of field values from (3·5) with the help of Tables III and IV. By such observations we can exclude various characteristic quadrupole arrays. As seen from those tables, $\tilde{\boldsymbol{Z}}_5'$, $\tilde{\boldsymbol{Z}}_4'$ and $\boldsymbol{Z}_5'$ have field values much lower than the others, though $\tilde{\boldsymbol{Z}}_3^0$ and $\tilde{\boldsymbol{Z}}_4^0$ have field values close to that of $\boldsymbol{Z}_5'$. The next lower field value comes from $\tilde{\boldsymbol{Z}}_2'$. The real quadrupole arrays with lower field values would include some of the above characteristic vectors with greater amplitudes. Results of our examination will be given below.

(A) We first take up $\tilde{\boldsymbol{Z}}_3^0$, $\boldsymbol{Z}_3^0$, $\tilde{\boldsymbol{Z}}_4'$, $\tilde{\boldsymbol{Z}}_5'$ and $\boldsymbol{Z}_5'$. In these characteristic arrays, both z_1 and z_2 vanish at all lattice points. Then z_3, z_4 and z_5 have magnitude of $(1/\sqrt{3})$ as seen from (3·10). This represents the molecular orientation with direction cosines $(\pm 1/\sqrt{3}, \pm 1/\sqrt{3}, \pm 1/\sqrt{3})$ except the choice of sign combinations. As seen from (3·11), two or none of z_3, z_4 and z_5 can change the signs simultaneously. Hence three of the characteristic arrays taken above should be combined in such a way that two of z_3, z_4 and z_5 might change their sign along a_2-axis of Fig. 1. This means that two of the characteristic arrays to be chosen should be of the $(0, \pi, 0)$ symmetry. For the same reason, two of them should be of the odd symmetry, in order that quadrupoles at both A- and B-lattice sites might be real. Keeping these in mind, we construct two real arrays

$$(1/\sqrt{3})\,(\tilde{\boldsymbol{Z}}_3^0+\tilde{\boldsymbol{Z}}_4'+\boldsymbol{Z}_5'),\quad (1/\sqrt{3})\,(\boldsymbol{Z}_3^0+\tilde{\boldsymbol{Z}}_4'+\tilde{\boldsymbol{Z}}_5'), \tag{3·12}$$

whose field values are respectively

$$\begin{aligned}(1/3)\,(\tilde{f}_3^0+\tilde{f}_4'+f_5') &= -24.00\,g,\\ (1/3)\,(f_3^0+\tilde{f}_4'+\tilde{f}_5') &= -18.18\,g.\end{aligned} \tag{3·13}$$

Here we used (3·5) with Tables III and IV. The first array in (3·12) has quite a low field value.

The arrays (3·12) do not satisfy the extremum conditions (3·8), of which the second and third equations are taken to be a set of independent conditions. Let us then assume a real quadrupole array given by

$$\boldsymbol{Z}=a_1^0\boldsymbol{Z}_1^0+a_2^0\boldsymbol{Z}_2^0+\tilde{a}_3^0\tilde{\boldsymbol{Z}}_3^0+\tilde{a}_4'\tilde{\boldsymbol{Z}}_4'+a_5'\boldsymbol{Z}_5'. \tag{3·14}$$

Decomposing our extremum conditions on the 8 lattice points into Fourier components, we get

$$-(f_1^0-\tilde{f}_4')\tilde{a}_4'a_1^0+\sqrt{3}(f_2^0-\tilde{f}_4')\tilde{a}_4'a_2^0+(\tilde{f}_3^0-f_5')a_5'\tilde{a}_3^0=0, \tag{3·15}$$

$$2(f_1^0-f_5')a_5'a_1^0-(\tilde{f}_3^0-\tilde{f}_4')\tilde{a}_4'\tilde{a}_3^0=0. \tag{3·16}$$

In these equations, (3·15) comes from the $(0, \pi, 0)$, odd component of the second equation of (3·8), and (3·16) from the $(0, \pi, 0)$, even component of the third equation of (3·8), where we used (3·4). There is no other Fourier component of the extremum conditions. It is clear from (3·15) and (3·16) that the first array in (3·12) does not satisfy the extremum conditions. It is also clear that the extremum array including $\tilde{\boldsymbol{Z}}_3^0$, $\tilde{\boldsymbol{Z}}_4'$ and $\boldsymbol{Z}_5'$ should be of the form (3·14); if we took into account the other characteristic arrays instead of $\boldsymbol{Z}_1^0$ and $\boldsymbol{Z}_2^0$, the $(0, \pi, 0)$, odd component of the second equation and $(0, \pi, 0)$, even component of the third one, both of (3·8), would remain unsatisfied.

In (3·15) and (3·16), $\tilde{a}_3^0$, $\tilde{a}_4'$ and a_5' are expressed in terms of a_1^0 and a_2^0 as given by (3·10):

$$\begin{aligned}\tilde{a}_3^0&=(1/\sqrt{3})\{(1-a_2^0-\sqrt{3}a_1^0)(1+2a_2^0)\}^{1/2},\\ \tilde{a}_4'&=(1/\sqrt{3})\{(1-a_2^0+\sqrt{3}a_1^0)(1+2a_2^0)\}^{1/2},\\ a_5'&=(1/\sqrt{3})\{(1-a_2^0)^2-3(a_1^0)^2\}^{1/2}.\end{aligned} \tag{3·17}$$

If we substitute (3·17) into (3·15) and (3·16), the results are two equations with respect to a_1^0 and a_2^0. The solution is given as follows:

$$\begin{aligned}a_1^0&=\frac{\sqrt{3}}{2}\frac{(\tilde{f}_3^0-\tilde{f}_4')(f_2^0-\tilde{f}_3^0-\tilde{f}_4'+f_5')}{(f_1^0-f_5')(3f_2^0-2\tilde{f}_3^0-2\tilde{f}_4'+f_5')-(\tilde{f}_3^0-\tilde{f}_4')^2},\\ a_2^0&=\frac{1}{2}\frac{(f_1^0-f_5')(-\tilde{f}_3^0-\tilde{f}_4'+2f_5')+(\tilde{f}_3^0-\tilde{f}_4')^2}{(f_1^0-f_5')(3f_2^0-2\tilde{f}_3^0-2\tilde{f}_4'+f_5')-(\tilde{f}_3^0-\tilde{f}_4')^2}.\end{aligned} \tag{3·18}$$

The above solution gives a real quadrupole array, satisfying the extremum condition. This solution is shown in the first row of Table VI.

Table VI. Real quadrupole arrays satisfying the extremum condition.

Label	Amplitudes of the characteristic arrays	Field value	Figure
(1)	$a_1^0=0.031$, $a_2^0=-0.006$, $\tilde{a}_3^0=0.560$, $\tilde{a}_4'=0.591$, $a_5'=0.580$	$-24.03\,g$	3 (a)
(2)	$a_1^0=0.165$, $a_2^0=0.108$, $a_3^0=0.464$, $\tilde{a}_4'=0.603$, $\tilde{a}_5'=0.618$	-20.28	3 (b)
(3)	$a_1^0=0.105$, $a_2^0=0.255$, $a_3'=0.419$, $\tilde{a}_4^0=0.485$, $\tilde{a}_5'=0.717$	-18.79	3 (c)
(4)	$\tilde{a}_1'=\tilde{a}_1''=\tilde{a}_1'''=-0.030$, $a_2^0=-0.125$, $\tilde{a}_2'=\tilde{a}_2''=\tilde{a}_2'''=0.413$, $\tilde{a}_5'=\tilde{a}_5''=\tilde{a}_5'''=0.396$	-21.68	4

In the same way we find two other arrays with lower field values, satisfying the extremum condition, as given in the second and third rows of Table VI. The molecular configurations corresponding to the above three quadrupole arrays are shown in Fig. 3. These are threefold degenerate, repectively.

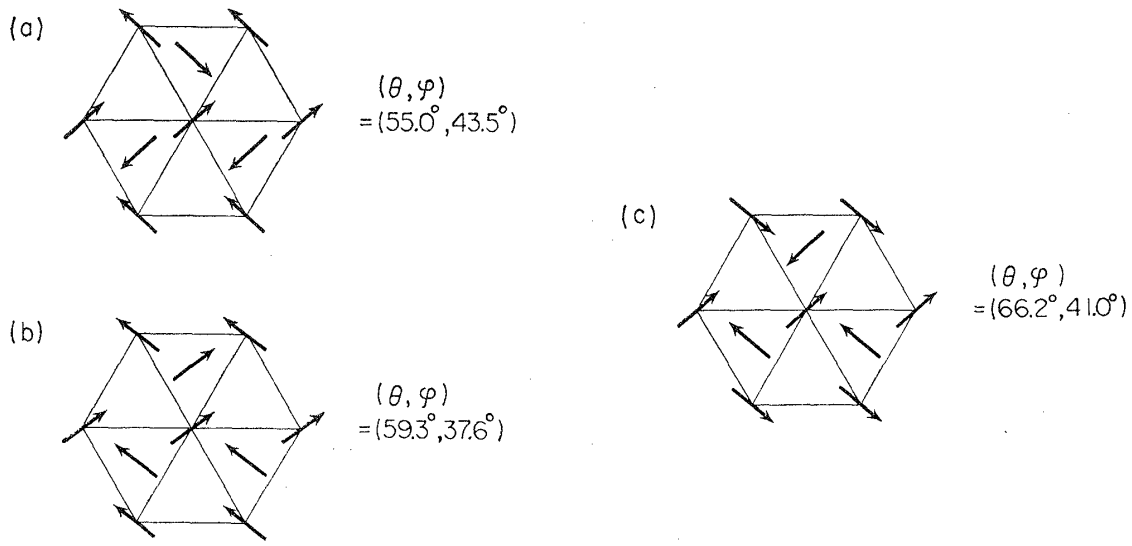

Fig. 3. Projection of molecular configurations given in Table IV.
(θ, φ) denote the polar and azimuthal angles of molecule at (0, 0, 0) site. The sense of projected vectors in c-plane represents the direction of molecule, the sign of ζ-component of direction cosines being fixed as positive.

(B) The arrays found in (A) do not include $\tilde{\boldsymbol{Z}}_2'$, $\tilde{\boldsymbol{Z}}_2''$ and $\tilde{\boldsymbol{Z}}_2'''$, which have a rather low field value. To complete our study, we examined some symmetrical arrays including the above characteristic arrays. First we could not find any extremum array with $\tilde{\boldsymbol{Z}}_2'$ and $\tilde{\boldsymbol{Z}}_1'$, being of low field value. Secondly, we examined arrays with $\tilde{\boldsymbol{Z}}_2''$, $\tilde{\boldsymbol{Z}}_2'''$, $\tilde{\boldsymbol{Z}}_1''$ and $\tilde{\boldsymbol{Z}}_1'''$, assuming $\tilde{a}_2''=\tilde{a}_2'''$ and $\tilde{a}_1''=\tilde{a}_1'''$. The lowest field value of the considered type is found to be $-17.19\,g$ after a troublesome analysis.

(C) Of quadrupole arrays with $\tilde{\boldsymbol{Z}}_2'$, $\tilde{\boldsymbol{Z}}_2''$ and $\tilde{\boldsymbol{Z}}_2'''$, we examine arrays of the following type:

$$\boldsymbol{Z}=\sum_{\mu=1,2,5}\{\tilde{a}_\mu'\tilde{\boldsymbol{Z}}_\mu'+\tilde{a}_\mu''\tilde{\boldsymbol{Z}}_\mu''+\tilde{a}_\mu'''\tilde{\boldsymbol{Z}}_\mu'''\}+a_2^0\boldsymbol{Z}_2^0. \tag{3·19}$$

In this type of arrays the third and fourth components of quadrupole, z_3 and z_4, vanish at all lattice points. As seen from (3·10), the array comes out if molecules are in c-plane ($z_2=-\frac{1}{2}$) or parallel to c-axis ($z_2=1$). From the extremum condition (3·8), we have now $z_5 f_1-z_1 f_5=0$ at the 8 lattice points, which are written in terms of the Fourier components

$$\begin{aligned}&(\tilde{f}_2'-\tilde{f}_5')\delta_1(\tilde{a}_2'\tilde{a}_5'+\tilde{a}_2''\tilde{a}_5''+\tilde{a}_2'''\tilde{a}_5''')\\&\qquad+(\tilde{f}_1'-\tilde{f}_5')\delta_2(\tilde{a}_1'\tilde{a}_5'+\tilde{a}_1''\tilde{a}_5''+\tilde{a}_1'''\tilde{a}'''_5)=0,\end{aligned} \tag{3·20a}$$

$$\begin{aligned}&(\tilde{f}_2'-\tilde{f}_5')\delta_1(\tilde{a}_2''\tilde{a}_5'''+\tilde{a}_2'''\tilde{a}_5'')\\&\qquad+(\tilde{f}_1'-\tilde{f}_5')\delta_2(\tilde{a}_1''\tilde{a}_5'''+\tilde{a}_1'''\tilde{a}_5'')\\&\qquad+\sqrt{3}(\tilde{f}_1'-\tilde{f}_2')\delta_1\delta_2(\tilde{a}_1''\tilde{a}_2'''-\tilde{a}_1'''\tilde{a}_2'')=0,\end{aligned} \tag{3·20b}$$

and the other two equations are generated from (3·20b) by cyclic permutations of $'$, $''$ and $'''$. There is no other Fourier component. In (3·20) we used the expressions for $\tilde{\boldsymbol{Z}}_\mu'$, $\tilde{\boldsymbol{Z}}_\mu''$ and $\tilde{\boldsymbol{Z}}_\mu'''$ given in Tables IV and V. The estimates of δ_1 and δ_2 are given also in Table IV. The extremum conditions (3·20) suggest a solution

$$\tilde{a}_\mu' = \tilde{a}_\mu'' = \tilde{a}_\mu''', \qquad \mu = 1,\ 2 \text{ and } 5,$$

for which (3·20) reduces to a single equation

$$\tilde{a}_5' \{ (\tilde{f}_2' - \tilde{f}_5') \delta_1 \tilde{a}_2' + (\tilde{f}_1' - \tilde{f}_5') \delta_2 \tilde{a}_1' \} = 0. \tag{3·21}$$

If we assume $\tilde{a}_5' \neq 0$, the solution of (3·21) brings a real quadrupole array with a field value $-21.68\,g$, as shown in Fig. 4. The numerical data are given in the fourth row of Table VI.

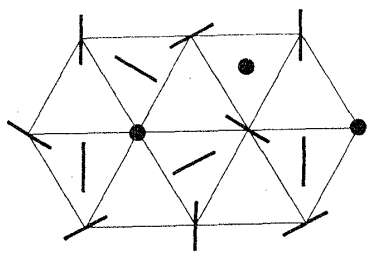

Fig. 4. Molecular configuration for the molecular array in the fourth row of Table IV.
Black circles represent molecules directed perpendicularly to c-plane. The other molecules lie in c-plane and rotate along hexagons surrounding the black circles, by a step of $\pi/3$, where the azimuthal angle of molecule at (1, 0, 0) site is $-32.3°$.

As a result of our examination, we conclude that the lowest real quadrupole array is given by Fig. 3(a) with the field value $-24.03\,g$. This configuration is included in the molecular patterns chosen by Kitaigorodskii and Mirskaya.[16] However, their method is not so systematic as given in the present paper. The other configurations they gave have high field values: they missed our solutions (2) and (4) given in Table VI. They missed also the lowest quadrupole configuration in fcc.

§ 4. Quantum mechanical correction to ground state energy

In the previous section we studied the classical quadrupole system in hcp. In the quantum mechanical quadrupole system, we interpret the molecular orientations resulting from the lowest classical solution as the quantized axes of molecules. Quantum mechanical expressions for quadrupole components are given in the column (b) of Table I. Those are the semi-diagonal part in $J=1$ with particular reference to ortho-hydrogens. The level spacing between $J=1$ and $J=3$ is quite large; we can neglect undoubtedly effects of the interaction non-diagonal in J on the ground state energy.

As the zeroth approximation, each ortho-molecule would be in the state $J_{\zeta'}=0$ in the frame of the quantized axes mentioned above, where ζ'-axes might be different for different molecules and $J_{\zeta'}$ denotes an eigenvalue of J_ζ referred to each quantized axis. In the oriented state $J_{\zeta'}=0$, the diagonal element of z_2 is $-2/5$, while that of the other z_μ vanishes. For this reason, the quadrupole

energy per molecule diagonal in $J_{\zeta'}$ would be half a field value multiplied by $(-2/5)^2$, for the lowest state. The estimates are given by

$$\begin{aligned} &\frac{1}{2}\left(-\frac{2}{5}\right)^2(-28.46\,g) = -4.65\,^\circ\mathrm{K}\ \ (\mathrm{fcc}),\\ &\frac{1}{2}\left(-\frac{2}{5}\right)^2(-24.03\,g) = -3.93\,^\circ\mathrm{K}\ \ (\mathrm{hcp}). \end{aligned} \tag{4·1}$$

Here $f(\mathrm{fcc}) = -28.46\,g$ is taken from reference 11). We note that Danielian's estimate for hcp[13] is $-0.74\,^\circ$K.

The above estimates for the ground state energies are semi-classical. There is a zero-point correction to them, as seen in the spin wave theory of antiferromagnets. This correction is generally small. However, the correction could be important, because we are concerned with a small difference of ground state energies for hcp and fcc ortho-hydrogens. The lowest energy in hcp is higher than that in fcc. This means that the state density of excitation spectra will be denser for hcp than for fcc, since the quadrupole energy averaged over all configurations is zero for both hcp and fcc. This observation suggests that the lowering of ground state energies due to the zero-point correction would be more appreciable for hcp than for fcc. A net effect will give a difference of ground state energies smaller than that predicted from (4·1).

We evaluate the zero-point correction by using a second order perturbation. The quadrupole interaction (2·2) is rewritten in the new coordinate system (ξ', η', ζ'), where ζ'-axes are taken to be respective quantized axes. We denote the orientation angles of the i-th quantized axis by (θ_i, φ_i). By a transformation $(\xi, \eta, \zeta) \to (\xi', \eta', \zeta')$, each quadrupole component is transformed as given by

$$z_\mu{}^i \to \sum_\nu T_{\mu\nu}(\theta_i, \varphi_i)\, z_\nu{}^{*i} \tag{4·2}$$

Table VII. Transformation matrix $T_{\mu\nu}(\theta, \varphi)$.

μ \ ν	1	2	3	4	5
1	$(1/2)(1+\cos^2\theta)\cdot\cos 2\varphi$	$(\sqrt{3}/2)\sin^2\theta\cdot\cos 2\varphi$	$-\sin\theta\sin 2\varphi$	$(1/2)\sin 2\theta\cdot\cos 2\varphi$	$-\cos\theta\sin 2\varphi$
2	$(\sqrt{3}/2)\sin^2\theta$	$(1/2)(3\cos^2\theta-1)$	0	$-(\sqrt{3}/2)\sin 2\theta$	0
3	$-(1/2)\sin 2\theta\cdot\sin\varphi$	$(\sqrt{3}/2)\sin 2\theta\cdot\sin\varphi$	$\cos\theta\cos\varphi$	$\cos 2\theta\sin\varphi$	$-\sin\theta\cos\varphi$
4	$-(1/2)\sin 2\theta\cdot\cos\varphi$	$(\sqrt{3}/2)\sin 2\theta\cdot\cos\varphi$	$-\cos\theta\sin\varphi$	$\cos 2\theta\cos\varphi$	$\sin\theta\sin\varphi$
5	$(1/2)(1+\cos^2\theta)\cdot\sin 2\varphi$	$(\sqrt{3}/2)\sin^2\theta\cdot\sin 2\varphi$	$\sin\theta\cos 2\varphi$	$(1/2)\sin 2\theta\cdot\sin 2\varphi$	$\cos\theta\cos 2\varphi$

with a transformation matrix shown in Table VII. In the new system, the quadrupole interaction (2·2) is written

$$W=\sum_{j>k}\sum_{\mu,\nu} z_\mu{}^{*j}\cdot F^*_{\mu\nu}(\boldsymbol{R}_j-\boldsymbol{R}_k)\cdot z_\nu{}^{*k}, \tag{4·3}$$

where

$$F^*_{\mu\nu}(\boldsymbol{R}_j-\boldsymbol{R}_k)=\sum_{\kappa,\sigma} T_{\kappa\mu}(\theta_j,\varphi_j)F_{\kappa\sigma}(\boldsymbol{R}_j-\boldsymbol{R}_k)T_{\sigma\nu}(\theta_k,\varphi_k). \tag{4·4}$$

We divide W into two parts

$$W=W^0+W', \tag{4·5}$$

where

$$W^0=\sum_{j>k} z_2{}^{*j}\cdot F^*_{22}(\boldsymbol{R}_j-\boldsymbol{R}_k)\cdot z_2{}^{*k} \tag{4·6}$$

and W' is the remaining part of W.

We want to regard W' as a perturbation with the unperturbed Hamiltonian W^0. However, in our choice of W^0 a trouble appears, as is seen if we analyze the quadrupole field vector $\boldsymbol{f}$ at each site. The field is written

$$\boldsymbol{f}=\phi_2\begin{pmatrix}0\\1\\0\\0\\0\end{pmatrix}+\phi_1\begin{pmatrix}1\\0\\0\\0\\0\end{pmatrix}+\phi_5\begin{pmatrix}0\\0\\0\\0\\1\end{pmatrix} \tag{4·7}$$

in the (ξ', η', ζ') system. The third and fourth components of $\boldsymbol{f}$ do not appear as a result of the extremum nature of the classical ground state. In (4·7) ϕ_2 is the field value, $\phi_1=\sum_k F^*_{12}(\boldsymbol{R}_j-\boldsymbol{R}_k)$ and $\phi_5=\sum_k F^*_{52}(\boldsymbol{R}_j-\boldsymbol{R}_k)$. ϕ_1 and ϕ_5 do not appear if the lowest characteristic array is real (fcc); the field is parallel to ζ'-axis and hence axially symmetric around ζ'-axis. This symmetry is broken in hcp. Due to different symmetries of the fields, we have different schemes of rotational levels, as shown in Fig. 5. The excited levels are splitted in hcp. On the other hand, W^0 of (4·6) gives doubly degenerate excited levels. However, the splitting given in Fig. 5 is very small compared with the excitation energy itself. There would be no appreciable error coming from our choice of W^0.

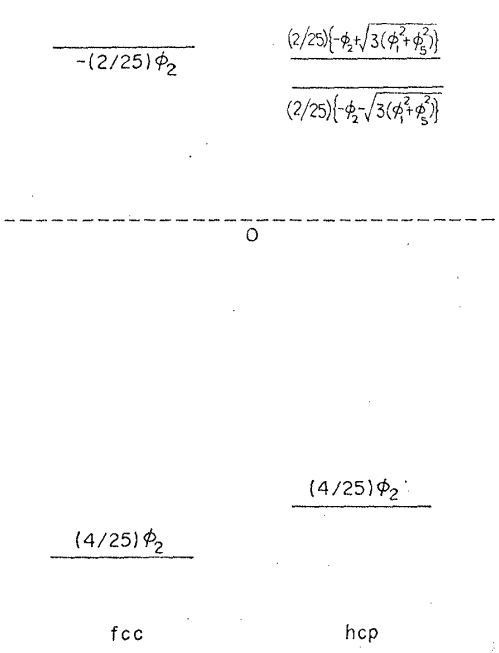

Fig. 5. Rotational levels in fcc and hcp under the field predicted from the classical ground state.
For fcc $\phi_1=\phi_5=0$, $\phi_2=-28.28\,g$.
For hcp $\phi_1=-0.355\,g$, $\phi_5=-1.369\,g$, $\phi_2=-24.03\,g$.

For the ground state $|0\rangle$ of W^0, all quadrupoles are in the state $J_{\zeta'}=0$. This approximate ground state is combined with states including the excitation of two molecules, j and k, through W'.

These states are

$$
\begin{aligned}
&\quad j\text{-th site} \quad k\text{-th site} \\
&|0, \cdots, +1, \cdots, +1, \cdots, 0\rangle = (1/2) J_+{}^j J_+{}^k |0\rangle, \\
&|0, \cdots, +1, \cdots, -1, \cdots, 0\rangle = (1/2) J_+{}^j J_-{}^k |0\rangle, \\
&|0, \cdots, -1, \cdots, +1, \cdots, 0\rangle = (1/2) J_-{}^j J_+{}^k |0\rangle, \\
&|0, \cdots, -1, \cdots, -1, \cdots, 0\rangle = (1/2) J_-{}^j J_-{}^k |0\rangle,
\end{aligned}
\tag{4·8}
$$

where $J_\pm = J_x \pm iJ_y$. Matrix elements relevant to perturbational calculations are the following:

$$
\begin{aligned}
&\langle 0, \cdots, 0, \cdots, 0, \cdots | W^0 | 0, \cdots, 0, \cdots, 0, \cdots\rangle \\
&\quad = (2/5)^2 \sum_{j>k} F^*_{22}(\boldsymbol{R}_j - \boldsymbol{R}_k) = (2/5)^2 (N/2) \phi_2 = W_0, \\
&\langle 0, \cdots, \pm 1, \cdots, \pm 1, \cdots | W^0 | 0, \cdots, \pm 1, \cdots, \pm 1, \cdots\rangle \\
&\quad = \langle 0, \cdots, \pm 1, \cdots, \mp 1, \cdots | W^0 | 0, \cdots, \pm 1, \cdots, \mp 1, \cdots\rangle \\
&\quad = W_0 + (2/5)^2 (3/2) \{-2\phi_2 + (3/2) F^*_{22}(\boldsymbol{R}_j - \boldsymbol{R}_k)\}, \\
&\langle 0, \cdots, \pm 1, \cdots, \pm 1, \cdots | W' | 0, \cdots 0, \cdots, 0, \cdots\rangle \\
&\quad = (2/5)^2 (3/8) [F^*_{44}(\boldsymbol{R}_j - \boldsymbol{R}_k) - F^*_{33}(\boldsymbol{R}_j - \boldsymbol{R}_k) \\
&\qquad\qquad \mp i \{F^*_{43}(\boldsymbol{R}_j - \boldsymbol{R}_k) + F^*_{34}(\boldsymbol{R}_j - \boldsymbol{R}_k)\}], \\
&\langle 0, \cdots, \pm 1, \cdots, \mp 1, \cdots | W' | 0, \cdots, 0, \cdots, 0, \cdots\rangle \\
&\quad = (2/5)^2 (3/8) [F^*_{44}(\boldsymbol{R}_j - \boldsymbol{R}_k) + F^*_{33}(\boldsymbol{R}_j - \boldsymbol{R}_k) \\
&\qquad\qquad \pm i \{F^*_{43}(\boldsymbol{R}_j - \boldsymbol{R}_k) - F^*_{34}(\boldsymbol{R}_j - \boldsymbol{R}_k)\}].
\end{aligned}
\tag{4·9}
$$

The energy correction from the second order perturbation becomes

$$
\begin{aligned}
W_2 &= -\sum_n \frac{|\langle n | W' | 0\rangle|^2}{W_n - W_0} \\
&= -(2/5)^2 (3/8) \sum_{j>k} \frac{1}{-2\phi_2 + (3/2) F^*_{22}(\boldsymbol{R}_j - \boldsymbol{R}_k)} \\
&\quad \times \{F^*_{44}(\boldsymbol{R}_j - \boldsymbol{R}_k)^2 + F^*_{33}(\boldsymbol{R}_j - \boldsymbol{R}_k)^2 + F^*_{43}(\boldsymbol{R}_j - \boldsymbol{R}_k)^2 \\
&\qquad + F^*_{34}(\boldsymbol{R}_j - \boldsymbol{R}_k)^2\}.
\end{aligned}
\tag{4·10}
$$

The classical ground configurations are shown in Fig. 6 for fcc and in Fig. 3(a) for hcp. With the help of them we evaluate $F^*_{\mu\nu}(\boldsymbol{R}_j - \boldsymbol{R}_k)$, which in turn enables us to evaluate W_2. In computations, we took into account only nearest neighboring pairs in the sum of (4·10); contributions from further neighbors decrease very rapidly as $|\boldsymbol{R}_j - \boldsymbol{R}_k|$ [10]. The result becomes

$$\frac{W_2}{N}=\begin{cases}-(2/5)^2\times 0.59\,g & \text{(fcc)},\\ -(2/5)^2\times 1.07\,g & \text{(hcp)}.\end{cases} \tag{4·11}$$

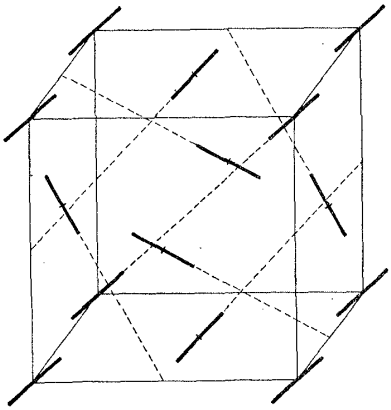

Fig. 6. Lowest molecular configuration in fcc. Each molecule points to a three-fold rotation axis as shown by broken lines.

(4·1) and (4·11) give our final result. The ground state energy per molecule is $-(2/5)^2\times 14.82\,g=-4.85\,°\mathrm{K}$ for fcc and $-(2/5)^2\times 13.09\,g=-4.28\,°\mathrm{K}$ for hcp. The energy difference proves to be 0.57 °K per molecule.*)

§ 5. Discussion

We have studied the lowest quadrupole configuration in hcp, which is constructed from the characteristic arrays with $\boldsymbol{\lambda}=(0,\pi,0)$, $(\pi,0,0)$ and $(\pi,\pi,0)$ with the help of the uniform arrays. One might ask if there may be some other characteristic arrays lower than our assumed ones. We give below some results of our examination concerning the above question. These are based on the field values resulting from the lattice sum taken up to nearest neighbors.

(A) *Field values of the characteristic arrays with* $\boldsymbol{\lambda}=(0,\pi,\pi)$

Field values are given by

$$-24.50\,g,\ -20.73\,g,\ -9.17\,g,\ 25.03\,g \text{ and } 29.37\,g,$$

where each value is doubly degenerate. Real quadrupole arrays constructed from these would not bring the lowest array.

(B) *Field values along* (0, 1, 0)*-axis in the Brillouin zone*

We studied the behavior of various field values along (0, 1, 0)-axis in the first Brillouin zone, namely as functions of $\boldsymbol{\lambda}=(0,\lambda,0)$. The result with the interaction taken up to nearest neighbors is shown in Fig. 7. As seen from the figure, the lowest field value appears at $(0,\pi,0)$. We also observe that the other two field values approach the lowest one with approaching $(0,\pi,0)$. This explains the reason why the lowest field value of the real quadrupole array appears at $(0,\pi,0)$. In Fig. 7 the accurate field values are shown also at two extremum points, (0, 0, 0) and $(0,\pi,0)$. The situation mentioned above would not change even if the accurate estimate was carried out.

We have concluded that fcc is more stable than hcp for ortho-hydrogens, with a stabilization energy of the quadrupole interaction, 0.57 °K per molecule. As mentioned in § 1, the para-hydrogen prefers hcp to fcc. This will be quite

*) See Note added in proof.

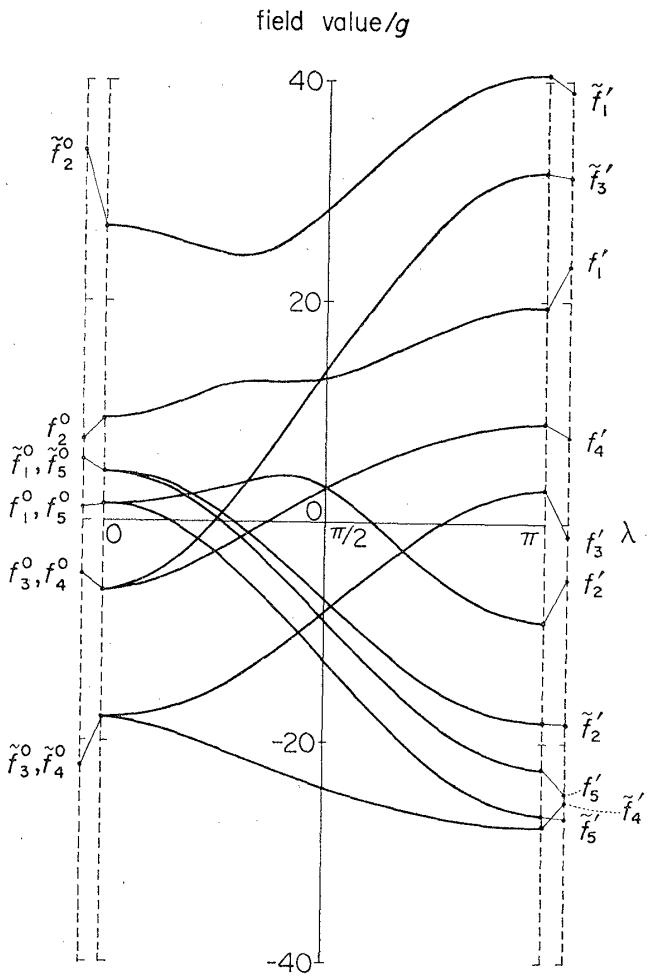

Fig. 7. Field values as functions of $\boldsymbol{\lambda}=(0, \lambda, 0)$.
The result is based on the lattice sum taken up to nearest neighbors. The accurate values with $\boldsymbol{\lambda}=(0, 0, 0)$ and $(0, \pi, 0)$ are marked outside by points, connected to the corresponding values with the nearest neighbor estimates.

a difficult problem to explain. Isenberg and Domb[20] tried to explain the relative stability of fcc and hcp crystals from the zero-point energy difference of lattice vibrations based on the harmonic approximation. They found the effect to be very small and concluded the anharmonic effect to be important in deciding the relative stability. In any way, our estimate of the stabilization energy of the quadrupole interaction, 0.57°K per molecule, gives an upper limit of the ground state energy difference of fcc and hcp para-hydrogens.

We finally note a point taken up by Raich and James.[18] They studied the temperature behavior of the molecular orientation in ordered fcc and hcp ortho-hydrogens, where the ordered configurations are assumed to be the N_2-pattern for fcc and the Kitaigorodskii-Mirskaya pattern for hcp. The configurations assumed are the correct choice; the lowest quadrupole array in fcc is of the N_2-type.[11] Raich and James found the orientation of molecules to be

dependent upon the temperature in hcp. Such a behavior comes out if the lowest characteristic array is fictitious. Because, near the transition temperature we have small average values of quadrupole components, which are free from the reality condition. The pattern of order parameters approaches the lowest fictitious array with approaching the transition temperature. In the sense of the Hartree approximation, the transition temperature is related to the lowest field value of characteristic arrays but not to that of real arrays.

Appendix

Quantum mechanical correction to quadrupolarization

The normalized perturbed state up to the second order is given by

$$|0) = |0\rangle + \sum_n \frac{\langle n|W'|0\rangle}{W_n - W_0}|n\rangle - \frac{1}{2}\sum_n \frac{|\langle n|W'|0\rangle|^2}{(W_n - W_0)^2}|n\rangle.$$

Then,

$$(0|\,\tfrac{3}{2}\,(J_{\zeta'}{}^j)^2 - 1|0) = -1 + \frac{3}{8}\sum_k \frac{1}{\{-2\phi_2 + \frac{3}{2}F_{22}^*(\boldsymbol{R}_j - \boldsymbol{R}_k)\}^2}$$
$$\times \{F_{33}^*(\boldsymbol{R}_j - \boldsymbol{R}_k)^2 + F_{34}^*(\boldsymbol{R}_j - \boldsymbol{R}_k)^2 + F_{43}^*(\boldsymbol{R}_j - \boldsymbol{R}_k)^2 + F_{44}^*(\boldsymbol{R}_j - \boldsymbol{R}_k)^2\},$$

whence we estimate the quadrupolarization to be

$$(0|\,\tfrac{3}{2}\,(J_{\zeta'})^2 - 1|0) = \begin{cases} -1 + 0.022 & \text{(fcc)}, \\ -1 + 0.048 & \text{(hcp)}. \end{cases}$$

References

1) M. Clouter and H. P. Gush, Phys. Rev. Letters **15** (1965), 200.
2) R. L. Mills and A. F. Schuch, Phys. Rev. Letters **15** (1965), 722.
3) J. Van Kranendonk and H. P. Gush, Phys. Letters **1** (1962), 22.
4) V. S. Kogan, A. S. Bulatov and L. F. Yakimenko, Soviet Phys.-JETP **19** (1964), 107.
5) R. W. Hill and B. W. A. Ricketson, Phil. Mag. **45** (1954), 277.
6) G. Ahlers and W. H. Orttung, Phys. Rev. **133** (1964), A1642.
7) F. Reif and E. M. Purcell, Phys. Rev. **91** (1953), 631.
8) S. A. Dickson and H. Meyer, Phys. Rev. **138** (1965), A1293.
9) T. Nakamura, Prog. Theor. Phys. **14** (1955), 135.
10) G. Grenier and D. White, J. Chem. Phys. **40** (1964), 3015.
11) O. Nagai and T. Nakamura, Prog. Theor. Phys. **24** (1960), 432; **30** (1963), 412 (Errata).
12) J. M. Luttinger and L. Tisza, Phys. Rev. **70** (1946), 954.
13) A. Danielian, Phys. Rev. **138** (1965), A282.
14) K. Tomita, Proc. Phys. Soc. (London) A **68** (1955), 214.
15) G. M. Bell and W. M. Fairbairn, Mol. Phys. **4** (1961), 481; **5** (1962), 605; **7** (1964), 497.
16) A. I. Kitaigorodskii and K. V. Mirskaya, Soviet Phys.-Cryst. **10** (1965), 121.
17) J. Felsteiner, Phys. Rev. Letters **15** (1965), 1025.
18) J. C. Raich and H. M. James, Phys. Rev. Letters **16** (1966), 173.
19) S. Homma, K. Okada and H. Matsuda, Prog. Theor. Phys. **36** (1966), 1310.

20) C. Isenberg and C. Domb, *Lattice Dynamics* (edited by R. F. Wallis, Pergamon Press, 1965).

Note added in proof: According to the computer result by Felsteiner[17] $f(\text{fcc}) = -28.28\,g$, which is supposed to be more reliable than ours. The resulting modification of (4·11) is negligibly small. If we take Felsteiner's value, the difference of the classical ground state energies for hcp and fcc is estimated to be 0.69°K, and that of the quantum mechanical ones 0.54°K, both per molecule.